ChemComm

Accepted Manuscript

This is an *Accepted Manuscript*, which has been through the Royal Society of Chemistry peer review process and has been accepted for publication.

Accepted Manuscripts are published online shortly after acceptance, before technical editing, formatting and proof reading. Using this free service, authors can make their results available to the community, in citable form, before we publish the edited article. We will replace this *Accepted Manuscript* with the edited and formatted *Advance Article* as soon as it is available.

You can find more information about *Accepted Manuscripts* in the **Information for Authors**.

Please note that technical editing may introduce minor changes to the text and/or graphics, which may alter content. The journal's standard **Terms & Conditions** and the **Ethical guidelines** still apply. In no event shall the Royal Society of Chemistry be held responsible for any errors or omissions in this *Accepted Manuscript* or any consequences arising from the use of any information it contains.

Journal Name

COMMUNICATION

Photocatalytic Hydrogen Evolution over β-Iron Silicide under Infrared-Light Irradiation

Masaharu Yoshimizu,[a] Ryoya Kobayashi,[a] Makoto Saegusa,[a] Toshihiro Takashima,[b] Hiroshi Funakubo,[c] Kensuke Akiyama,[d] Yoshihisa Matsumoto[d] and Hiroshi Irie*[b,e]

We investigated the ability of β-iron silicide (β-FeSi$_2$) to serve as a hydrogen (H$_2$)-evolution photocatalyst due to the potential of its conduction band bottom, which may allow thermodynamically favorable H$_2$ evolution in spite of its small band-gap of 0.80 eV. β-FeSi$_2$ had an apparent quantum efficiency for H$_2$ evolution of ~ 24% up to 950 nm (near infrared light), in the presence of dithionic acid ion (S$_2$O$_6^{2-}$) as a sacrificial agent. It was also sensitive to infrared light (>1300 nm) for H$_2$ evolution.

Since the first report of the Honda-Fujishima effect regarding photo-induced water splitting by titanium dioxide (TiO$_2$) electrodes,[1] the use of photoelectrodes and powdered photocatalysts to convert solar energy into hydrogen (H$_2$) gas has been extensively investigated.[2] Suitable photocatalysts for solar-to-H$_2$ reactions require the following characteristics: 1) a band-gap smaller than ~ 2 eV, 2) negative potential of the conduction band (CB) bottom compared to H$^+$/H$_2$ potential (0 V vs. SHE), and 3) high stability in aqueous solution following light irradiation.[3] However, it is difficult to satisfy these three requirements with conventional oxides, as their valence band (VB), which is predominantly composed of oxygen (O) 2p orbitals, has a top potential of 2.94 V (vs. SHE) typically.[4] Thus, the CB bottom of such oxides is more positive than H$^+$/H$_2$ potential, meaning they do not produce H$_2$ under solar-light irradiation.

A number of strategies to decrease the band gap of active oxide photocatalysts have been pursued. A common method involves the doping of foreign elements into wide band-gap oxide photocatalysts to form impurity levels in the forbidden band.[5] Oxide photocatalysts with smaller band-gaps can also be produced without dopants using specific d^{10} or d^{10}s^2 metal ions with closed electronic shell configurations, such as Ag$^+$, Cu$^+$, In^{3+}, and Bi^{3+}, to shift the VB top to a more negative region.[6] Another approach is to generate nitride, oxynitride, sulfide, or oxysulfide compounds, which also have VB tops that are more negative than that of O 2p, as these VBs consist of nitrogen (N) 2p, hybrid N 2p/O 2p, sulfur (S) 3p, and hybrid S 3p/O

2p orbitals, respectively.[7, 8] Recently, we reported that ZnRh$_2$O$_4$, which has a band-gap of 1.2 eV, functions as an H$_2$-evolution photocatalyst in spite of the open electronic shell configuration of Rh^{3+} (d^6 configuration). Ligand-field splitting in octahedrally coordinated Rh^{3+} forms fully occupied t$_{2g}^6$ and empty e$_g^0$ orbitals that comprise the VB top and CB bottom, respectively, resulting in a pseudo-closed electronic shell configuration.[3] In this configuration, the VB top potential is much more negative (~ 0.1 V vs. SHE) than that of typical oxides, and the CB bottom potential is more negative than that needed for H$_2$ evolution.

Here, except for oxide, nitride (oxynitride) and sulfide (oxysulfide) compounds, we attempted to identify a new type of H$_2$ evolution photocatalyst that is composed of abundant, chemically stable, and non-toxic elements. Specifically, we focused on β-FeSi$_2$ as a candidate photocatalyst for H$_2$ evolution because it possesses a small band-gap (0.80 eV) and a work function of 4.65 eV,[9] suggesting that its CB bottom potential is more negative than H$^+$/H$_2$ potential, allowing for thermodynamically favorable H$_2$ evolution.

Commercial β-FeSi$_2$ powder (Soekawa Rikagaku, purity, 99%) was pulverized using a planetary ball-milling apparatus at 500 rpm for 10 min before use (Figs. S1a and S1b in ESI-1† and Figs. S2a and S2b in ESI-2†). 150-nm-thick β-FeSi$_2$ thin films were deposited on a silver (Ag)-coated silicon (100) substrate using a metal organic chemical vapor deposition (MOCVD) method (ESI-3†)[10].
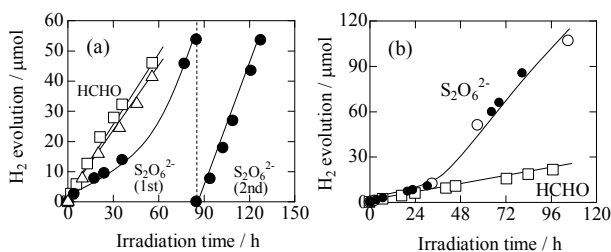
β-FeSi$_2$ is unstable in basic solutions and generates H$_2$ according to the reaction: Si + 2OH$^-$ + H$_2$O → SiO$_2$ + 2H$_2$. For this reason, the pH dependence of its stability in dark conditions was evaluated by measuring H$_2$ evolution at various pHs (Fig. S3 in ESI-4†). As expected based on the above equation, a large amount of H$_2$ was detected at pH 10. At pH 7, H$_2$ evolution was largely reduced, and at pH 3 and 4, H$_2$ evolution was negligibly small, indicating that the photocatalyst was stable under these acidic pH conditions. Notably, however, H$_2$ evolution was unexpectedly detected at pH 1 at a similar level to that observed at pH 7 (ESI-4†). For this reason, the

H$_2$ evolution properties of β-FeSi$_2$ in response to visible light were evaluated at pH 3.

Figure 1a shows the concentration of H$_2$ evolved by β-FeSi$_2$ under visible-light irradiation (> 560 nm) in the presence of either S$_2$O$_6^{2-}$ (0.3 M) or HCHO (0.1 M) as a sacrificial agent (ESI-5[†]). Under both conditions, a relatively large amount of H$_2$ was produced. These results are plausible because photo-excited holes in the VB of β-FeSi$_2$ are consumed during the oxidation of S$_2$O$_6^{2-}$ and HCHO, allowing for the photo-excited electrons in the CB to reduce H$_2$O and produce H$_2$. An induction period for H$_2$ evolution was observed only in the case of S$_2$O$_6^{2-}$ in the first cycle of light irradiation; however, this delay was not observed in the second cycle (ESI-5[†]). Notably, H$_2$ evolution was detected under light irradiation at wavelengths larger than 1300 nm in the presence of either S$_2$O$_6^{2-}$ or HCHO, indicating that β-FeSi$_2$ is sensitive to infrared light (Fig. 1b). The reproducibility of this reaction was confirmed using newly pulverized β-FeSi$_2$ in the presence of S$_2$O$_6^{2-}$.

β-FeSi$_2$ utilized in the present study functioned as a p-type semiconductor (ESI-3[†]). According to the 4.65-eV work function of β-FeSi$_2$, which corresponds to ~ 0.15 V vs. SHE, and the 0.80-eV band gap of β-FeSi$_2$, the VB top and CB bottom potentials of β-FeSi$_2$ were estimated to be ~ 0.15 and ~ -0.65 V vs. SHE, respectively, on condition that the Fermi level is equal to the VB top potential. Thus, photo-generated electrons in the CB of β-FeSi$_2$ can thermodynamically reduce H$_2$O, resulting in H$_2$ evolution (ESI-5[†]).

We also examined the wavelength dependence of the apparent quantum efficiency (AQE) for H$_2$ evolution by β-FeSi$_2$ (Fig. 2a, ESI-5[†]). The UV-visible diffuse reflectance spectrum of β-FeSi$_2$ and distribution of the irradiating monochromatic light are also shown in Figs. 2a and 2b, respectively. With increasing wavelength of monochromic light, the AQE values were unchanged between 440±10 and 950±25 nm. N otably, the changes in the AQE values coincided well with the UV-visible spectrum over this wavelength range. Although the maximum wavelength of irradiating light that could be examined was 1000 nm due to the specifications of the spectroradiometer, the constant AQE values for H$_2$ evolution from 440±10 to 950±25 nm are reasonable due to the constant light-absorption capability of β-FeSi$_2$.

Finally, we examined the stability of under light conditions in aqueous solution at pH 3 (ESI-6[†]). The surface of as-deposited β-FeSi$_2$ was mainly composed of O, Si^{4+} and Si^0, and Fe^0 was only detected in low amounts, indicating that the main surface component of the β-FeSi$_2$ thin film was O-Si-O and Si (0 h, Fig. 3a; and 0 nm, Figs. 3b-3e). After dark storage in aqueous solution (pH 3 and 0.1 M HCHO) for 24 h, the amounts of surface O, Si-species (Si^0, Si^{2+}, and Si^{4+}), and Fe^0 were not markedly changed (Fig. 3a). Under xenon light irradiation in solution, Si^0 and Fe^0 slightly decreased, Si^{2+} and O slightly increased, and Si^{4+} remained constant after 24-h irradiation (48 h in x-axis, Fig. 3a), indicating that the β-FeSi$_2$ thin film surface was partially oxidized. However, during further irradiation for 12 h (60 h in x-axis, Fig. 3a), the amounts of Si^0, Si^{2+}, Si^{4+}, Fe^0, and O remained constant, indicating that the surface became stable with continued irradiation.
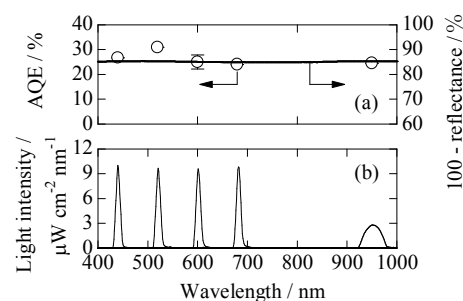
Fig. 2 Dependence of AQE (plots) on the wavelength of irradiating monochromatic light. H$_2$ evolution was observed at pH 3 in the presence of S$_2$O$_6^{2-}$. UV-visible diffuse reflectance spectrum (solid line) of β-FeSi$_2$ is also shown (a). Distributions of the irradiating monochromatic light at 440, 520, 600, 680±10 and 950±25 nm are shown. A controlled of light intensity of ~ 100 μW/cm^2 was used for each wavelength (b).
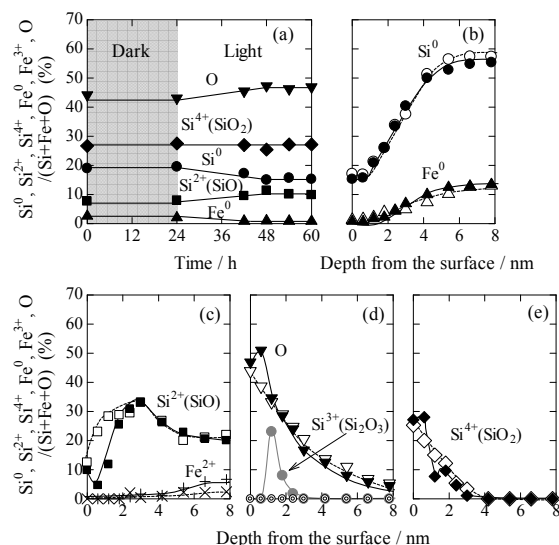
Fig. 3 Percentages of Si^0, Si^{2+}, Si^{3+}, Si^{4+}, Fe^0, Fe^{2+} and O at the surface of as-deposited β-FeSi$_2$ thin film before and after dark storage, and after xenon-light irradiation at the indicated intervals (a). Depth profiles showing the percentage of Si^0 and Fe^0 (b) Si^{2+} and Fe^{2+} (c), Si^{3+} and O (d), and Si^{4+} (e) in the β-FeSi$_2$ thin film after xenon-light irradiation (closed symbols and plus marks) and for the as-deposited thin film (open symbols, double circles, and cross marks).

Fig. 1 Changes in H$_2$ concentration by water splitting as a function of time over β-FeSi$_2$ photocatalyst under irradiation with visible light (>560 nm) (a) and infrared light (>1300 nm) (b) in the presence of either S$_2$O$_6^{2-}$ (solid and open black circles) or HCHO (open black squares and triangles) as a sacrificial agent. The reaction in (a) with S$_2$O$_6^{2-}$ was allowed to proceed for 128 h with evacuation after 85 h. That in (a) with HCHO was repeated twice with newly pulvarized β-FeSi$_2$ to confirm the reproducibility of the photocatyltic reaction. In (b), the reaction in the presence of S$_2$O$_6^{2-}$ was also repeated twice with newly pulverized β-FeSi$_2$ to confirm the reproducibility.

The depth profiles of Si^0, Si^{2+}, Si^{4+}, Fe^0, and O, as well as Si^{3+} and Fe^{2+}, on the β-$FeSi_2$ thin film in the as-prepared state and in aqueous solution after 36 h xenon-light irradiation were examined and compared (Figs. 3b-3e). The depth profiles of Si^{2+}, Si^{3+}, Si^{4+}, and O differed between the light-irradiated and as-deposited films within ~ 2 nm from the surface, whereas those of Si^0, Fe^0 (without bonding to O), and Fe^{2+} did not markedly change after light irradiation. Specifically, the amount of Si^{2+} was higher, and that of Si^{4+} and O was lower in the as-deposited thin film. This result is reasonable because oxidized species decrease with increasing depth from the surface, meaning that O-Si-O (Si^{4+}) and Si-O (Si^{2+}) bonds decreased and increased, respectively. In contrast, the amounts of Si^{3+}, Si^{4+}, and O increased at the surface, but then decreased, whereas Si^{2+} decreased at surface, but then increased with increasing depth. The behavior of these species is plausible because the surface of β-$FeSi_2$ (up to ~ 2 nm depth) was oxidized after irradiation with light. However, at depths greater than ~ 2 nm from the surface, the percentages of Si^0, Si^{2+}, Si^{3+}, Si^{4+}, Fe^0, Fe^{2+}, and O were similar between the β-$FeSi_2$ thin films before and after light irradiation. Notably, the ratio of Fe^0 to Si^0 was less than 0.5 in spite of the composition of $FeSi_2$, even up to a depth of 8 nm in the film. This may have been due to a difference in the etching rate of Fe and Si, as Fe would be more easily etched. Moreover, although Si^{4+} was completely undetectable, the O species (SiO, Si_2O_3, and O) remained in the β-$FeSi_2$ thin film in the as-prepared state and that after light irradiation. Although the reasons for this difference are unknown, it is possible that O was initially present in the β-$FeSi_2$ thin film or O was incorporated into the film during the etching process. Despite the presence of O species, the oxidized layer of the film did not exceed ~ 2 nm, indicating that the β-$FeSi_2$ photocatalyst becomes chemically stable by forming such oxides (ESI-7[†]). A similar phenomenon was reported with $TiSi_2$, which was covered a layer of oxides with a thickness of 2-5 nm and also exhibited chemical stability.[11]

Conclusions

We demonstrated that under irradiation with the entire range of UV and visible light, as well as infrared light up to 950±25 nm, β-$FeSi_2$ evolves H_2 in the presence of either $S_2O_6^{2-}$ or HCHO by band-gap photo-excitation. Notably, β-$FeSi_2$ is also capable of utilizing infrared light longer than 1300 nm to produce H_2, which, to our knowledge, is the longest wavelength of light to be utilized by an H_2-evolution photocatalyst. Although β-$FeSi_2$ has a small band-gap (0.85 eV), its VB top (~ 0.58 V vs. SHE) lies at a potential markedly more negative than that of conventional oxides, and its CB bottom (~ –0.28 V vs. SHE) lies at potential more negative than that of H^+/H_2, allowing for thermodynamically favorable H_2 evolution. Notably, it was also demonstrated that sulfate ion (in the present study, $S_2O_6^{2-}$) can be utilized in this system as a sacrificial agent. As $S_2O_6^{2-}$ is regarded as a water pollutant, this β-$FeSi_2$-based H_2 evolution system could also address environmental concerns in addition to generating H_2 energy, as it could potentially remove sulfate ions from water. Such investigations are currently being conducted in our laboratory.

Notes and references

[a] Interdisciplinary Graduate School of Medicine and Engineering, University of Yamanashi, 4-3-11 Takeda, Kofu, Yamanashi 400-8511, Japan

[b] Clean Energy Research Center, University of Yamanashi, 4-3-11 Takeda, Kofu, Yamanashi 400-8511, Japan

[c] Department of Innovative and Engineering Materials, Tokyo Institute of Technology, 4259 Nagatsuda, Midori-ku, Yokohama, Kanagawa 266-8502, Japan

[d] Kanagawa Industrial Technology Center, 705-1 Shimoizumi, Ebina, Kanagawa 243-0435, Japan

[e] Japan Science and Technology Agency (JST), Core Research for Evolutionary Science and Technology (CREST), 5 Sanbancho, Chiyoda-ku, Tokyo 102-0075, Japan

† Electronic Supplementary Information (ESI) available: SEM images; UV-visible absorption spectrum; Preparation of β-$FeSi_2$ thin films and electrical conducting type of β-$FeSi_2$, pH dependence of the stability; Procedures and comments for photocatalytic water-splitting: Procedures of testing stability using XPS; TEM images. See DOI: 10.1039/c000000x/

1   A. Fujishima and K. Honda, *Nature*, 1972, **238**, 37.
2   K. Maeda, K. Teramura, D. Lu, T. Takata, N. Saito, Y. Inoue and K. Domen, *Nature*, 2006, **440**, 295; H. Kato, H. Kobayashi and A. Kudo, *J. Phys. Chem. B.*, 2002, **106**, 12441-12447; K. Sayama, K. Mukasa, R. Abe, Y. Abe and H. Arakjawa, *J. Photo. Photo. A: Chem.*, 2002, **148**, 71; X. Wang, K. Maeda, A. Thomas, K. Takanabe, G. Xin, J. M. Carlsson, K. Domen and M. A. Antonietti, *Nature Mater.*, 2009, **8**, 76.
3   Y. Takimoto, T. Kitta and H. Irie, *Int. J. Hydro. Ener.*, 2012, **37**, 134.
4   S. D. Scaif, *Solar Ener.*, 1980, **25**, 41.
5   H. Kato and A. Kudo, *J. Phys. Chem. B*, 2002, **106**, 5029; T. Ishii, H. Kato and A. Kudo, *J. Photochem. Photobiol., A*, 2004, **163**, 181.
6   Y. Maruyama, H. Irie and K. Hashimoto, J. Phys. Chem. B, 2006, 110, 23274; J. W. Tang, Z. G. Zou and J. Ye, *Chem. Mater.*, 2004, **16**, 1644; J. W. Tang, Z. G. Zou and J. Ye, *Angew. Chem. Int. Ed.*, 2004, **43**, 4463.
7   M. Hara, G. Hitoki, T. Takata, J. N. Kondo, H. Kobayashi and K. Domen, *Stud. Surf. Sci. Catal.*, 2003, **145**, 169; M. Hara, G. Hitoki, T. Takata, J. N. Kondo, H. Kobayashi and K. Domen, *Catal. Today*, 2003, **78**, 555; A. Kasahara, N. Nukumizu, T. Takata, J. N. Kondo, M. Hara, H. Kobayash and K. Domen, *J. Phys. Chem. B*, 2003, **107**, 791.
8   A. Ishikawa, T. Takata, J. N. Kondo, M. Hara, K. Kobayashi and K. Domen, *J. Am. Chem. Soc.*, 2002, **124**, 13547; I. Tsuji, H. Kato, H. Kobayashi and A. Kudo, *J. Am. Chem. Soc.*, 2004, **126**, 13406; I. Tsuji, H. Kato and A. Kudo, *Angew. Chem. Int. Ed.,* 2005, **44**, 3565; H. Kaga, K. Saito and A. Kudo, *Chem. Commun.*, 2010, **46**, 3779.
9   I. Nishida, *Phys. Rev. B*, 1973, **7**, 2710: D. Leong, M. Harry, K. J. Reeson, and K. P. Homewood, *Nature*, 1997, **387**, 686.
10 K. Akiyama, S. Motomura, K. Hayashi, H. Funakubo and M. Itakura, *Phys. Status Solidi C*, 2013, **10**, 1684; S. Motomura, K. Hayashi, M. Itakura, K. Akiyama, *Phys. Status Solidi C*, 2013, **10**, 1815.
11 P. Ritterskamp, A. Kuklya, M. A. Wustkamp, K. Kerpen, C. Weidenthaler and M. Demuth, *Angew. Chem. Int. Ed.*, 2007, **46**, 7770.

Graphical abstract
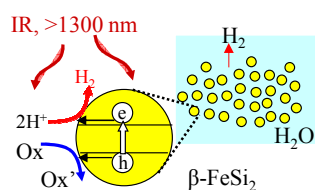
Photocatalytic Hydrogen Evolution over β-Iron Silicide under Infrared-Light Irradiation

Masaharu Yoshimizu, Ryoya Kobayashi, Makoto Saegusa, Hiroshi Funakubo, Kensuke Akiyama, Yoshihisa Matsumoto and Hiroshi Irie

We investigated the ability of β-FeSi$_2$ (0.80 eV) to serve as a hydrogen (H$_2$)-evolution photocatalyst, sensitive to infrared light (>1300 nm).